A generalized model of human body radiative heat exchanges for optimal design of indoor thermal comfort conditions

A generalized model of human body radiative heat exchanges for optimal design of indoor thermal comfort conditions

Concettina Marino[a], Antonino Nucara[a], Giorgia Peri[b,1] , Matilde Pietrafesa[a], Gianfranco Rizzo[b]

[a] *Department of Civil, Energy, Environmental and Material Engineering (DICEAM), 'Mediterranea' University of Reggio Calabria, Reggio Calabria, Italy*

[b] *Department of Energy, Information Engineering, and Mathematical Models (DEIM), University of Palermo, Palermo, Italy*

Abstract

Human thermal sensation depends heavily on radiative exchanges between the human body and the surrounding environment. Because these exchanges play a crucial role in the thermal balance of the human body, about 35% of the process, human thermal sensation should draw the attention of planners when designing both indoor environments and equipment.

The present study aims to contribute to this field by proposing a procedure for delineating the optimal comfort conditions for occupants in most of the articulate and realistic configurations of actual indoor environments. Specifically, this procedure enables accurate assessment of the radiant field surrounding a subject in a given indoor realistic environment and considers its variability with space and time along with the presence of high-intensity radiant sources. The proposed simulation tool contains a set of algorithms in which the degree of complexity depends on the level of accuracy for modelling the radiative heat transfer between the occupants and surrounding environment.

The feasibility of these algorithms for designers and researchers has also been checked for a single room characterised by the presence of windows in two different exposures. This configuration implies a complex pattern of the sun entering the room, which in turn determines relevant spatial modifications of the indoor comfort thermal conditions. Such complex situations are effectively interpreted by the proposed model.

[1] Corresponding author. Email: peri@dream.unipa.it

This analysis provides useful indications for suitable design of layouts of the confined space and the size of an effective heating, ventilating, and air conditioning system to limit the discomfort felt inside the room.

Keywords

Thermal comfort; Radiative exchange; Projected area factors; View factors

1 Introduction

The current conventional wisdom is that comfort and energy demands in buildings are closely interrelated. Thus, the efforts for designing efficient buildings are focused on the accomplishment of the primary objective of edifices: to provide shelter and comfort for people who live, work, and interact in them (CEN, 2007). However, modern constructions must comply with laws and standards specifically designed with the aim of both minimising the energy consumptions of buildings and meeting basic comfort requirements (EU, 2010; ISO, 2005; CEN, 2007). The achievement of proper comfort levels is also binding for energy efficiency purposes (Roulet, 2001). In fact, occupants usually tend to react to any perceived discomfort by taking actions to restore their comfort, but sometimes these actions may increase energy costs. Therefore, it is important to recognise that a 'low energy' standard that increases occupant discomfort may be no more sustainable than another one encouraging energy use (Nicol and Humphreys, 2002).

From this point of view, thermal comfort can be considered as the most relevant aspect of the issue because it directly affects both building energy performance and occupant productivity in indoor environments (d'Ambrosio et al., 2011; Seppänen et al., 2006). Its assessment involves a series of environmental parameters and subjective variables which must be accurately evaluated (d'Ambrosio et al., 2014; Dell'Isola et al., 2012), and the values must be kept within the recommended or prescribed parameters (CEN, 2007). Among these factors, radiative heat exchanges play a pivotal role. In moderate confined environments, they contribute up to 30% of the entire thermal exchange involving a subject (La Gennusa et al., 2005). Moreover, they can become the most significant cause of indoor heat gain and discomfort in the presence of direct solar radiation (Thellier et al., 2008; Marino et al., 2017a; Marino et al., 2017b).

It is widely established that the building envelope has a crucial influence on radiative heat fluxes involving the human body and that this aspect should be properly considered in the building design stage.

Nevertheless, this is not an easy task because typical façades are composed of different components such as windows, walls, and shading devices which may exert different and sometimes opposite influences on the indoor thermal comfort conditions of occupants. Moreover, it is worthy to note that along with the influence of the façade's features - that are more and more characterized by innovative components (Bianco et al., 2017) -, comfort conditions in actual environments also depend on human behaviour (Andersen et al., 2013; Fabi et al. 2012; Marino et al, 2015a).

Therefore, to properly manage the involved parameters and to make the building design phase effective, coded procedures and methodologies need to be implemented so that radiative human body heat exchange and the related comfort conditions can be correctly assessed by suitably considering indoor environment configurations and occupants' positions.

Several algorithms are available in literature that extensively analyse single aspects of thermal comfort. Among them, simulation of radiation for thermal comfort (Stratbücker, 2013) and modelling of short-wave solar radiation for comfort effects (Arens et al., 2015) are methods employed most often, along with estimation of the operative temperature for a subject under direct sunlight (Karlsen et al., 2014). Despite these efforts, however, comprehensive procedures are not available for predicting indoor thermal comfort conditions by correctly considering the geometry of the confined environment and envelope features such as wall temperature and window position and dimension, particularly in the presence of direct solar radiation on the position occupied by the subject. The availability of such comprehensive procedures would be highly useful for supporting building designers and technicians in fulfilling their task of correctly estimating the building envelope size and an appropriate effective heating, ventilating, and air conditioning (HVAC) system in a twofold attempt toward minimising the energy consumption for indoor environment climatisation and providing comfortable conditions for the occupants. In fact, inaccurate definitions of the spatial and time changes of the indoor thermal balance of occupants and the radiative heat exchange would likely result in ineffective sizes and positions of climatisation systems. Particularly in commercial buildings, where occupancy is expected for lengthy periods in the same position inside a particular room, poor knowledge of the spatial variability of the comfort conditions would result in less effective utilisation of the indoor spaces.

The present study approaches this limitation by providing an all-inclusive set of algorithms that considers occupant preferences such as clothing and activity; indoor parameters utilised for controlling HVAC systems including air temperature, air relative velocity, and partial pressure of vapour; and parameters linking the

position of people inside a room with the building layout including wall surface temperature, the presence of radiant heat sources and direct or diffuse solar radiation, the projected area factors, and occupant position. These algorithms also consider time and the predicted spatial changes in global thermal comfort, such as the Predicted Mean Vote (PMV) and Predicted Percentage of Dissatisfied people (PPD), along with local discomfort conditions including radiant asymmetry. The outcome is obtained through intermediate assessment of the indoor radiant field by computing the mean and plane radiant temperatures. In this way, radiative heat transfer between occupants and the surrounding environment can be modelled for any complex geometrical situation and for any radiant source affecting occupants regardless of their positions in the room.

By using the calculation tool introduced in this study, the effect of the building structure on indoor thermal comfort can be modelled in a time-changing regime and in different zones of the room's floor rather than merely in steady-state average conditions to enable complete mapping of the spatial variation of the occupants' indoor thermal conditions. This is particularly important in buildings characterised by complex geometry, where the mean radiant temperature (MRT) and the radiant asymmetry vary inside rooms, or in the presence of direct solar radiation on the subject.

This comprehensive approach is a new contribution for overcoming existing methods referring to single aspects of thermal comfort. It presents an effective tool for designers to easily obtain useful information concerning the indoor performances of buildings at the design stage and offers positive implications in practice.

2 Indoor human body radiative exchange

Thermal sensations are generally related to the response of the human body to the surrounding thermal environment. During the past few decades, many thermo-physiological models have been developed to predict the human thermal response as a function of both physiological parameters and variables defining the surrounding environment (Marino et al., 2017b). Usually based on energy balance equations of the human body, such models differ from each other (Fanger, 1970; Katic et al., 2014; Tanabe et al., 2002; Fengzhi, 2005; Fiala et al., 2012; Fiala et al., 2001; Huizenga et al., 2001; Zhang et al., 2004) in the patterns used to model the body itself and for the hypothesised time regime, whether steady or transient. Therefore, the human body's balance equation assumes a key role in the assessment of indoor thermal comfort. The

following sections outline the structure of the steady-state heat balance equation, upon which one of the most widely used model is based (ISO, 2005; ASHRAE, 2010).

The steady-state human body's balance equation (Fanger, 1970) is yielded from the application of the first law of thermodynamics and is given by

$$\Delta S = (M - W) - (C_{res} + E_{res} + C + R + E_d + E_{sw}), \quad (1)$$

where ΔS is the time change in internal energy; M is metabolic heat production; W is mechanical power; C_{res}, C, and R are dry heat losses by dry respiration, convection and radiation, respectively; and E_d and E_{sw} are latent heat losses owing to vapour diffusion through the skin and evaporation of sweat, respectively.

Except for E_{sw}, all of the thermal losses appearing in eq. (1) depend on a set of subjective, physical, and physiological independent parameters according to the scheme in Table 1, where I_{cl} is the thermal insulation of clothing, t_a is air temperature, v_a is air velocity, $\bar{t}_r$ is the MRT of the surrounding environment, p_a is water vapour partial pressure, and t_{sk} is skin temperature. The definition of each involved parameter can be found in (ISO, 2001).

Table 1. Parameters involved in the terms of the human body thermal balance equation.

Terms appearing in the thermal balance equation		**Physical and physiological parameters**							
		M (W)	I_{cl} (m²°C/W)	t_a (°C)	v_a (m/s)	$\bar{t}_r$ (°C)	p_a (Pa)	t_{sk} (°C)	E_{sw} (W)
Metabolic power	M	✓							
Mechanical power	W	✓							
Respiratory convective heat loss	C_{res}	✓		✓					
Respiratory evaporative heat loss	E_{res}	✓					✓		
Convective heat loss	C	✓	✓	✓	✓				
Radiative heat loss	R		✓			✓			
Diffusion heat loss	E_d		✓					✓	
Evaporation of sweat heat loss	E_{sw}								✓

Regarding the contribution of each thermal loss to the body's thermal balance, it is worthy of note that in the most frequent actual configurations of indoor environments, the share of the radiative exchange is often prevalent. For example, by applying the balance eq. (1) to a typically occurring situation of a subject normally clothed for the season of the year (I_{cl}= 0.5 clo in winter and 1.0 clo in summer) performing a sedentary activity (M =1.2 met) inside a thermally uniform environment (i.e. air velocity of 0.1 m/s, humidity ratio of 50%, air and MRT of 20°C in winter and 26°C in summer), the results given in Table 2

were obtained. These results imply that the radiative heat exchange, with a share of about 35%, plays a crucial role in the thermal balance of the human body and therefore should draw the attention of planners when designing both indoor environment and equipment. For this reason, the radiant field should be accurately considered when either the room or the correspondent building façade is configured (ISO, 2001; Parson, 2014; La Gennusa et al., 2007).

Table 2. Typical contribution of various thermal losses to the body's balance equation.

Heat loss	Winter		Summer	
	W/m^2	%	W/m^2	%
Breathing (sensible)	1.4	2%	0.8	1%
Breathing (latent)	5.6	7%	5.0	8%
Convection	25.1	33%	19.2	31%
Radiation	26.9	35%	21.8	35%
Perspiration	12.4	16%	10.9	17%
Sweating	4.9	6%	4.9	8%

Specifically, considering the human subject as a small body in a large cavity, the radiative heat exchange from the subject to the environment may be evaluated if the MRT is known.

Because it is determined by the indoor environment configuration and by the occupant's position inside a room, the MRT is a pivotal factor in assessing the effect of the radiant field on human thermal response (Parson, 2014) and therefore in the correct design of enclosed space, systems, and working positions.

In the following sections, according to the indoor conditions experienced by the human body, pertinent algorithms are given for computing the relevant parameters needed for assessing the main factors affecting the radiative heat exchange: MRT, radiant asymmetry, projected area factors, and view factors. This set of algorithms, simultaneously utilised, will delineate a general and comprehensive procedure for properly modelling the radiative heat exchange of the human body.

3 Mean radiant temperature: a general expression

The MRT has been defined as 'the uniform temperature of an imaginary black enclosure in which an occupant would exchange the same amount of radiant heat as in the actual non-uniform enclosure (ISO, 2001). This parameter is exploited to assess the radiative heat exchange occurring between the occupants and

the internal surfaces of the building envelope, which actually have different temperatures. Within this context, it is worth noting that every surface, including the human body, performs differently when affected by either short- or long-wave radiant fluxes. Therefore, the radiative balance of the body, and consequently the MRT, must consider this difference.

Short-wave radiation is generally produced by high-intensity sources, such as those characterised by a small area, a high emission temperature, and a strongly directional beam. Sun radiation can be considered among these radiant sources. Because it may strongly affect the radiant field and the MRT, sun radiation is often a significant cause of discomfort to people (La Gennusa et al., 2007; Hodder and Parsons, 2006; Marino et al., 2015b); therefore, the contribution of this source must be properly assessed.

The following sections introduce the proper algorithms to enable calculation of the MRT in all possible situations involving solar radiation.

The radiative net energy lost by the human body, Q_S, inside an enclosed cavity can be evaluated as the difference between the flow emitted by the subject, Q_{0S}, and the absorbed ratio of the thermal flow that reaches the subject, $Q_{A\to S}$ (Figure 1).

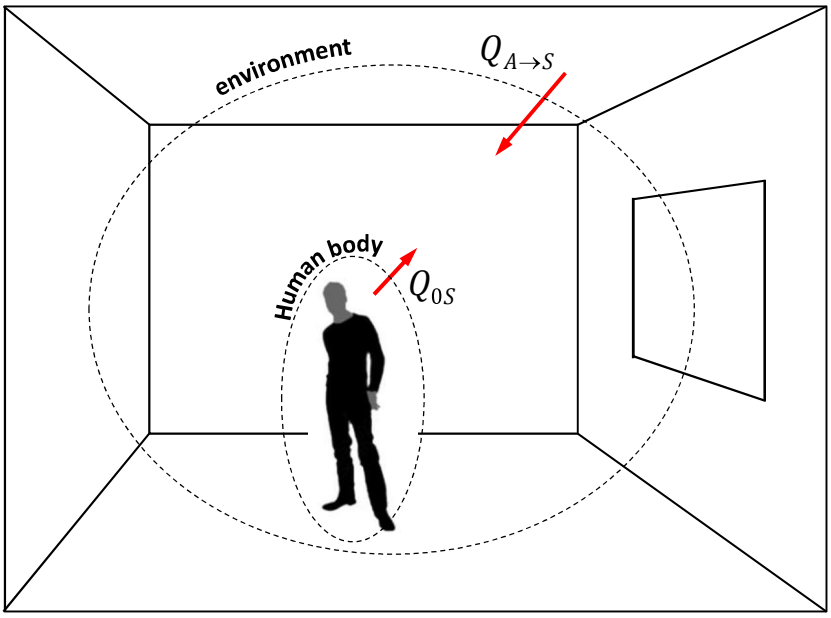

Figure 1. Typical radiative exchange between the human body and the building envelope.

The latter term is a function of the thermal radiation coming from the surfaces of the surrounding environment, $Q_{A\to S}$ (Kreith et al., 2011). However, such high-intensity sources may consistently alter the

radiant field to cause significant human discomfort. To pattern the effects of their presence, we need to consider the share of the high-intensity energy flux (short wave), $Q_{ir\to S}$, which is absorbed by the subject.

Because the sun can be deemed as a high-intensity source, this effort should also be considered to assess the MRT in the case of a subject irradiated by solar radiation. Solar radiation includes two components, direct $Q_{d\to S}$ and diffuse $Q_{b\to S}$, which must be treated differently because their features are different. One is highly directional, and the other is not; therefore, they perform in different ways when entering the indoor environment through windows, and their radiative exchanges with the human body are different (La Gennusa et al., 2007).

Following these considerations, in the more general case, we can write

$$Q_S = Q_{0S} - \alpha_S Q_{A\to S} - \alpha_{irr} Q_{ir\to S} - \alpha_{irr}(Q_{d\to S} + Q_{b\to S}), \tag{2}$$

where α_S is the absorbance of the human body, and α_{irr} is the absorbance of the outer surface of the human body at the actual average wavelength of the high-intensity radiative energy flux reaching the subject.

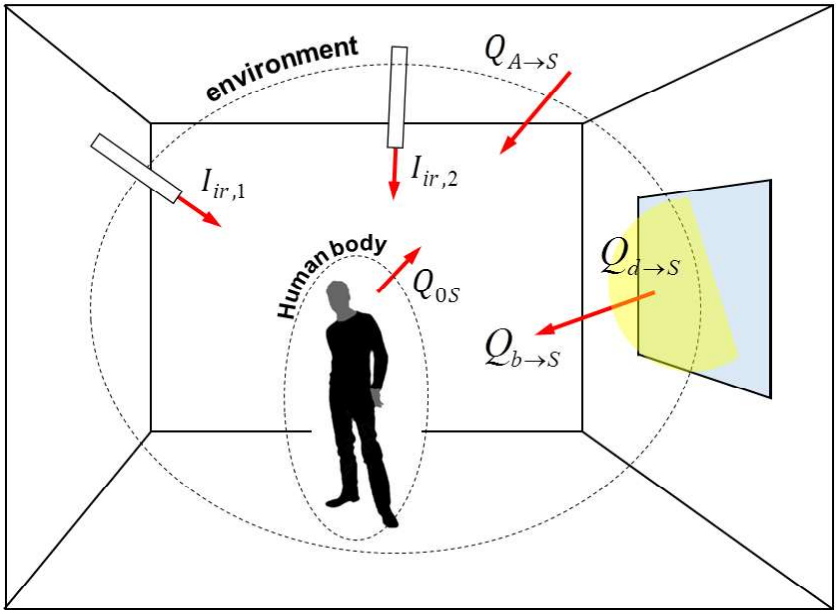

Figure 2. Radiative exchange between the human body and the building envelope in presence of solar radiation.

The radiative heat flow Q_{0S} emitted by the subject can be written as

$$Q_{0S} = \sigma \varepsilon_S A_r T_{cl}^4, \tag{3}$$

where σ is the Stefan–Boltzmann constant; ε_S is the emittance of the person; A_r is the effective radiation area of the person, or the smallest convex surface enveloping the human bod;, and T_{cl} is the (absolute) mean temperature of the clothed surface of the human body.

In the hypothesis that the internal surfaces of the building can be considered as black bodies, characterised by emissivity $\varepsilon_i = 1$ and reflectance $\varrho_i = 1 - \varepsilon_i = 0$, the total radiation coming from the surfaces surrounding the environment and received by the subject can be expressed as

$$Q_{A\to S} = \sigma A_r \sum_{i=1}^{N} F_{S\to i} T_i^4, \tag{4}$$

where $F_{S\to i}$ is the angle factor between the subject and the i^{th} internal surface of the envelope, T_i is the temperature of the i^{th} surface of the envelope, and N is the number of the involved isothermal surfaces.

$Q_{ir\to S}$ can be evaluated as

$$Q_{ir\to S} = \sum_{j=1}^{M} A_{p,j} I_{ir,j}, \tag{5}$$

where I_{ir} is the intensity of the radiation coming from the j^{th} high-intensity energy source, A_p is the projected area of the subject onto a plane perpendicular to the direction of the incoming flux, and M is the number of high-intensity energy sources.

Finally, in the hypothesis that the diffuse radiation entering the room through the glazed surfaces follows Lambert's law, the incidence of this component of solar radiation on the subject can be evaluated by the following expression:

$$Q_{d\to S} = A_r \sum_{j=1}^{N_g} F_{S\to j} I_{d,j}, \tag{6}$$

where $F_{S\to j}$ is the angle factor between the human body and the j^{th} glazed surface, $I_{d,j}$ is the intensity of the diffuse radiation entering the room through the j^{th} glazed surface, and N_g is the number of glazed surfaces.

On the contrary, the radiative flux owing to the direct component of the solar radiation on the subject can be obtained by the equation

$$Q_{b\to S} = A_p I_b, \tag{7}$$

where A_p is the projected area of the subject onto a plain normal to the direction of the solar beam, and I_b is the intensity of the direct radiation striking the subject.

By considering the previous equations and referring to Kirchhoff's law, in which $\alpha_S = \varepsilon_S$, it is possible to rewrite eq. (2) as

$$Q_S = \sigma\varepsilon_S A_r T_{cl}^4 - \sigma\varepsilon_S A_r \sum_{i=1}^{N} F_{S\to i} T_i^4 - \alpha_{irr}\left(\sum_{j=1}^{M} A_{p,j} I_{ir,j} + A_r \sum_{j=1}^{N_g} F_{S\to j} I_{d,j} + A_p I_b\right). \quad (8)$$

Moreover, because the human body is surrounded by an enclosed environment, the net flux leaving the human body (Q_S) must be equal to the flux exchanged by radiation between the human body and the surfaces of the environment ($Q_{S\leftrightarrow A}$) of the subject; that is:

$$Q_S = Q_{S\leftrightarrow A}. \quad (9)$$

The calculation of $Q_{S\leftrightarrow A}$ can be derived under the following hypotheses: The environment is an enclosure with a uniform temperature $\bar{T}_r$ (MRT); the temperature of the human body is equal to the mean temperature of its clothed surface, T_{cl}; and the human body is significantly smaller than the dimensions of the surrounding environment. In this case, the thermal radiative flow exchange between a subject and the surrounding surfaces of the enclosed environment is given by

$$Q_{S\leftrightarrow A} = \sigma\varepsilon_S A_r\left(T_{cl}^4 - \bar{T}_r^4\right). \quad (10)$$

Considering eqs. (8), (9), and (10), the following relationship can be defined:

$$\sigma\varepsilon_S A_r T_{cl}^4 - \sigma\varepsilon_S A_r \sum_{i=1}^{N} F_{S\to i} T_i^4 - \alpha_{irr}\left(\sum_{j=1}^{M} A_{p,j} I_{ir,j} + A_r \sum_{j=1}^{N_g} F_{S\to j} I_{d,j} + A_p I_b\right) = A_r\sigma\varepsilon_S\left(T_{cl}^4 - \bar{T}_r^4\right), \quad (11)$$

which once solved yields the more general expression of the MRT:

$$\bar{T}_r = \sqrt[4]{\sum_{i=1}^{N} F_{S\to i} T_i^4 + \frac{\alpha_{irr}}{\varepsilon_s\sigma}\left(\sum_{j=1}^{M} f_{p,j} I_{ir,j} + \sum_{j=1}^{N_g} F_{S\to j} I_{d,j} + f_p I_b\right)}, \quad (12)$$

where $f_p = A_p/A_r$ is the projected area factor.

In the case of a non-irradiated subject, the MRT is given by

$$\bar{T}_r = \sqrt[4]{\sum_{i=1}^{N} F_{S\to i} T_i^4}. \quad (13)$$

In the presence of high-intensity radiant sources without the presence of sun, the formula becomes

$$\bar{T}_r = \sqrt[4]{\sum_{i=1}^{N} F_{S\to i} T_i^4 + \frac{\alpha_{irr}}{\varepsilon_s\sigma}\sum_{j=1}^{M} f_{p,j} I_{ir,j}}. \quad (14)$$

Finally, in the case of a subject irradiated by only solar radiation, we have

$$\bar{T}_r = \sqrt[4]{\sum_{i=1}^{N} F_{S\to i} T_i^4 + \frac{\alpha_{irr}}{\varepsilon_s\sigma}\left(\sum_{j=1}^{N_g} F_{S\to j} I_{d,j} + f_p I_b\right)}. \quad (15)$$

It is worth noting that one of the main hypotheses upon which previous equations rely regards the internal surfaces of the building, which are assumed to behave as black bodies. However, when solar radiation

occurs, this hypothesis is not completely feasible (ASHRAE, 1989), and the reflected component of the radiation should therefore be considered.

In such a case, the following relationship can be derived (Marino, 2017a):

$$\overline{T}_r = \sqrt[4]{\sum_{i=1}^{N} F_{S\to i} T_i^4 + \frac{\alpha_{irr}}{\varepsilon_S \sigma}\left[\sum_{j=1}^{N_g} F_{S\to j} I_{dj} + f_p I_b + \sum_{i=1}^{N} \rho_i \left(\sum_{j=1}^{N_g} F_{i\to j} I_{dj}\right) F_{S\to i} + 0.5\, \rho_{floor} I_{bh}\right]}, \qquad (16)$$

where ρ_i is the reflectance of the i^{th} surface of the envelope, $F_{j\to i}$ is the angle factor between the j^{th}glazed surface and the i^{th} opaque surface of the building envelope, ρ_{floor} is the reflectance of the floor, and I_{bh} is the direct radiation that strikes the horizontal surface of the pavement.

The relationships formerly reported show that depending on both geometrical parameters (view factors, projected area factors) and time-changing factors (surface temperature and solar radiation), the MRT is characterised by spatial and temporal variability which cannot be neglected in most of the actual cases. Therefore, assessment of the needed parameters must be conducted in a transient regime including various subject positions inside the confined space.

Clearly, consideration of the sun's effect requires a geometrical definition of each relevant point and surface of the room with respect to the position of the solar radiation at the needed time step. Specifically, in correspondence to each time step, the floor area irradiated by the sun is defined by geometric considerations (La Gennusa et al., 2007), thus ascertaining whether the equation for a non-irradiated or irradiated subject must to be used.

4 Radiant asymmetry: definition and assessment

Local thermal discomfort, an adverse thermal response of the body to the surrounding thermal environment, is often solicited by undesired local cooling or heating of a specific area of the body. The main causes of local discomfort are air temperature gradients, non-homogeneous floor temperatures, air drafts, and asymmetric thermal radiation (ISO, 2005; Fanger, 1970; Beccali et al., 2004). The latter is generally caused by the presence of excessively hot or cold surfaces or other heat sources which may alter the uniformity of the radiant field surrounding the subject. Consequently, different parts of the body, with different exposures, might reach different temperatures, which in turn may cause sensations of discomfort.

To assess indoor environments from this point of view, ISO standards (ISO, 2005; ISO, 1998) have devised a method based on the asymmetry of the plane radiant temperature (Δt_{pr}) which considers the difference between the plane radiant temperature for each side of two opposite faces of a small plane element (ISO, 2001) and the related PPD (ISO, 2005; Fanger et al., 1985). The plane radiant temperature (t_{pr}) is defined as the uniform temperature of an enclosure where the radiative flux on one side of a small plane element, the so called 'test area', is the same as that in the actual environment (ISO, 2001). For the assessment of local discomfort, both horizontal and vertical plane asymmetries must be evaluated; therefore, the radiant temperature asymmetry is calculated with reference to three orthogonal directions. As a result, three plane elements respectively orthogonal to the X, Y, and Z axes (Figure 3) must be considered; hence, six test areas including one for each side of the plane elements must also be considered.

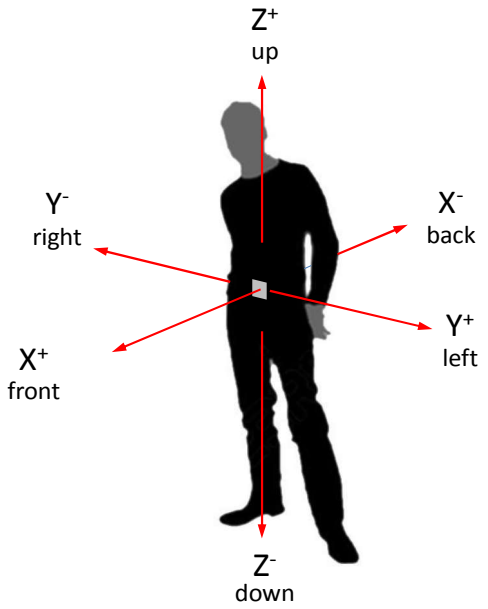

Figure 3. Reference system feasible for the calculation of the plane radiant asymmetry.

The plane radiant temperature can be calculated as follows (ISO, 1998):

$$T_{pr} = \sqrt[4]{\sum_{i=1}^{N} F_{AT\to i} T_i^4}, \tag{17}$$

where T_i is the temperature of the i^{th} isothermal surface of the environment, and $F_{AT\to i}$ is the view factor between the test area and the i^{th} isothermal surface.

The relationship reported in ISO (1998) considers only long-wave radiation fluxes; therefore, when short-wave radiation fluxes occur, the formula must be modified to properly pattern their effect. This case was

analysed by researchers (Marino et al., 2017b) who exploited a rationale similar to that leading to eq. (15). In that case, the expression describing the plane radiant temperature (17) was revised to consider the influence of the various components of the solar radiation:

$$T_{pr} = \sqrt[4]{\frac{\alpha_{AT}}{\varepsilon_{AT}} \sum_{i=1}^{N} F_{AT \to i} T_i^4 + \frac{\alpha_{irr}}{\sigma \varepsilon_{AT}} \left(\sum_{j=1}^{M} F_{AT \to j} I_{d,j} + I_{b\perp} \right)}, \quad (18)$$

where $F_{AT \to j}$ is the view factor between the test area and the j^{th} glazed surface, I_d is the intensity of the diffuse solar radiation from the sky, and $I_{b\perp}$ is the component of the beam solar radiation perpendicular to the surface of the test area. The absorption coefficients α_{AT} and α_{irr} refer to infrared and solar radiation, respectively; and ε_{AT} represents the emittance of the test area.

5 Algorithms for calculating the relevant anthropometric parameters

As evidenced by the previous algorithms, thermal radiative exchange of the human body with surrounding surfaces depends strongly on radiation data referring to human body anthropometry. This set of data is composed mainly of the body surface area, clothing area factor, effective radiation area factor, and projected area factor. Several analytical and experimental methods may be utilised to compute these parameters. A detailed description of the most common methodologies used for determining these and other various relevant anthropometric parameters are reported in (Nucara et al., 2012), which includes the results of field analysis conducted by employing an experimental apparatus.

The following sections summarise the main algorithms needed for calculating the anthropometric parameters (i.e. the projected area factor and view factor) relevant for assessing both MRT and radiant asymmetry.

5.1 Projected area factor

The projected area factor describes which part of a body's subject is irradiated from a given point (Figure 4), thus enabling assessment of the contribution of radiative fluxes coming from high-intensity sources to the radiative energy balance of the human body. It is defined as

$$f_p = \frac{A_p}{A_r}, \quad (19)$$

where A_p is the projected area of the subject onto a plain normal to the direction of the radiative flux, and A_r is the effective radiation area of the person. The latter is the area emitting and receiving radiation from the surroundings, or the smallest convex surface enveloping the human body. Because parts of the body do not exchange radiation with the surroundings (e.g. zones under the arms), this area is smaller than the total area of the body.

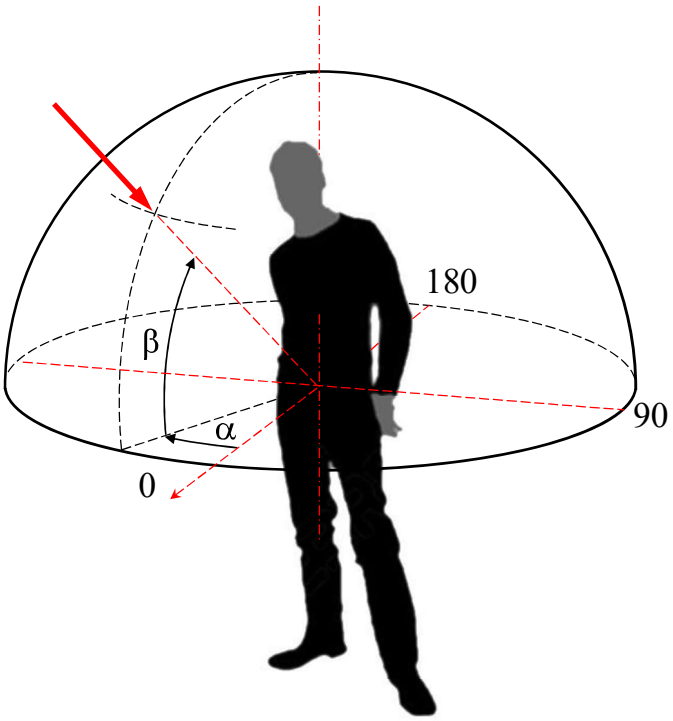

Figure 4. Azimuth, α, and altitude, β, angles.

As determined by the human silhouette, the value of the projected area factor changes with the subject's posture (usually standing or seated) and depends on the relative position of the point of view to the person, or the location of the source. This in turn is identified by two angles, azimuth α and altitude β, as illustrated in Figure 4. Original data reported in Figure 5 were obtained by Fanger (Fanger, 1970), who used a photographic method for different directions identified by angles α and β. In this case, the projected area factor, $f_p(\alpha, \beta)$, was obtained as the ratio between the projected area, $A_p(\alpha, \beta)$, and the effective radiating area of the human body.

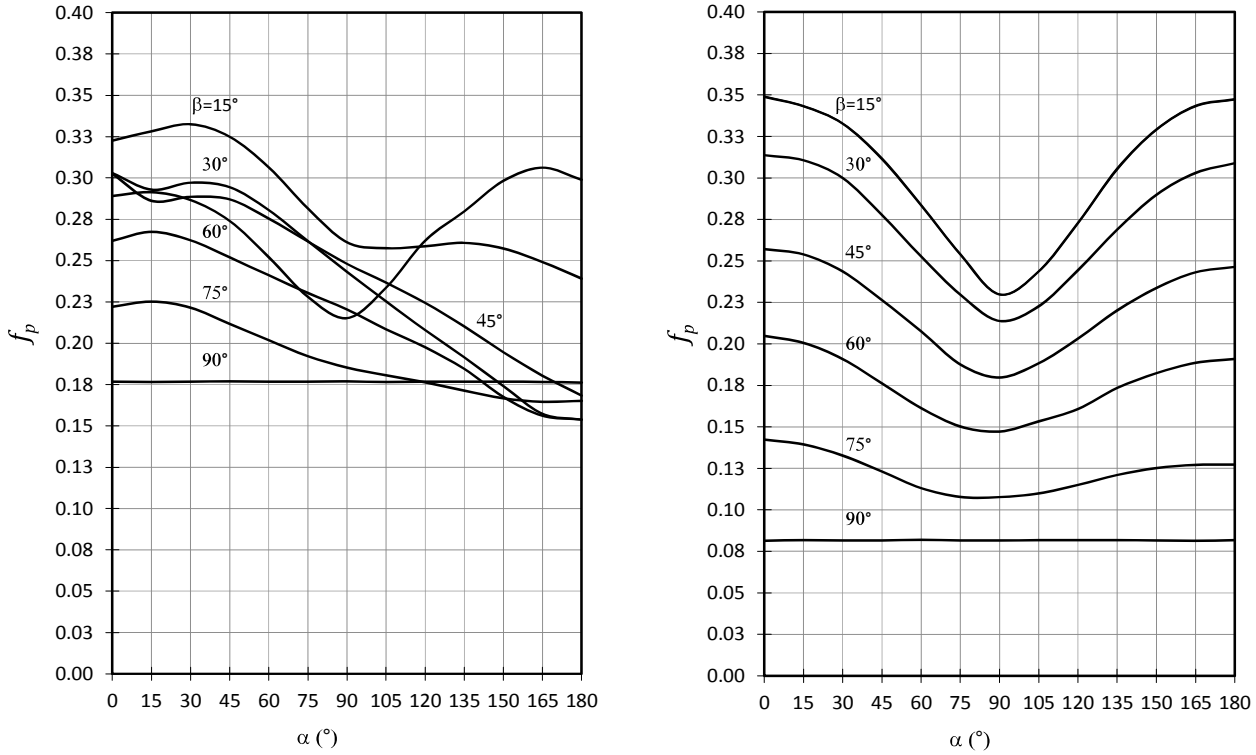

Figure 5. Projected area factors for people standing (left) and seated (right) (Fanger, 1970).

Fanger's original data were verified with several different methodologies and for people of different genders or ethnic groups (Horikoshi et al., 1990; Miyazaki et al., 1995). An experimental photographic apparatus that can obtain more pictures of subjects at smaller angle steps is developed in (La Gennusa et al., 2008; Calvino et al., 2005).

To analytically assess the projected factor, Fanger's original data were interpolated (Rizzo et al., 1991). The obtained equations are among the most reliable and most often utilised (Vorre et al., 2015):

$$f_p(\alpha, \beta) = \sum_{i=0}^{4} \sum_{j=0}^{3} A_{ij} \alpha^i \beta^j, \tag{20}$$

where coefficients A_{ij} are available in (Rizzo et al., 1991) for both seated and standing people.

5.2 View factors

To calculate the radiant energy exchanges between a person and the enveloping environment, a set of pivotal parameters is needed that includes the surface temperatures of the subject and the surrounding surfaces, their emissivity, and pertinent view factors.

The view factor represents the fraction of the diffusely distributed radiation that leaves the surface of the human body and reaches another surface. The following sections report algorithms suitable for calculating view factors in the most frequently occurring configurations of actual environments.

5.2.1 View factors between human body and rectangular surfaces characterised by tilted and rotated angles

The envelope structures of most actual enclosed environments are characterised by rectangular shapes. In this case, to derive the relations enabling view factor calculation, the reference system depicted in Figure 6 must be considered.

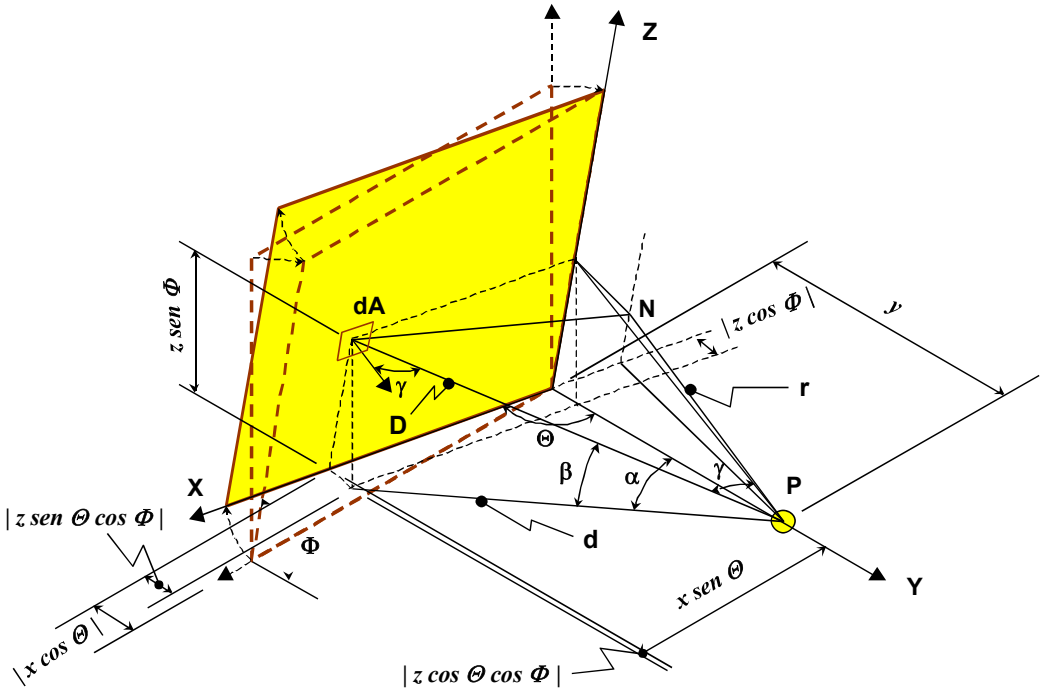

Figure 6. Reference system and geometrical parameters used for view factor assessment when the subject (P) is facing the rectangular surface A, tilted at angle Φ, and swivelled at angle Θ.

Specifically, the subject is expected to be located at the position indicated by point P, which has coordinates (0,c,0), and faces the origin (0,0,0); moreover, the rectangular surface, which is in front of the subject, is sized ($a \times b$), rotated at angle Θ, and tilted at angle Φ. Considering the infinitesimal element dA of the surface A, according to the view factor reciprocity rule, the following relation can be written as

$$A_r \, dF_{P \to dA} = dA \, F_{dA \to P}, \tag{21}$$

where $dF_{P \to dA}$ is the view factor between the subject, and dA, $F_{dA \to P}$ is the view factor between the element dA and the subject, whose effective area is A_r.

On the contrary, for the definition of view factor

$$dF_{dA \to P} = \int_P dF_{dA \to dP} \tag{22}$$

is

$$dF_{dA \to dP} = \frac{q_{dA \to dP}}{q_{0dA}}, \tag{23}$$

where $q_{dA \to dP}$ is the radiant flux emitted by dA and striking the infinitesimal element dP of the subject's surface, and q_{0dA} is the total radiant flux emitted by dA.

Under the assumption that the surface A is a source complying with Lambert's law, it is possible to obtain

$$q_{dA \to dP} = I_n \frac{\cos\gamma \cos\delta}{D^2} dA\, dP, \tag{24}$$

where I_n is the intensity of the radiation, γ is the angle between the line orthogonal to dA and the direction $dA \to dP$, and δ the angle between the line orthogonal to dP and the line segment connecting dA to dP, the length of which is D.

Moreover, with a perfectly diffusing surface (complying with Lambert's law), dA emits the following radiative flow:

$$q_{0dA} = \pi I_n dA. \tag{25}$$

Thus, by exploiting eqs. (24) and (25) in (23):

$$dF_{dA \to dP} = \frac{\cos\gamma \cos\delta}{\pi D^2} dP. \tag{26}$$

Hence, by integrating over the area of the subject,

$$\int_P dF_{dA \to dP} = \frac{\cos\gamma}{\pi D^2} A_p, \tag{27}$$

where A_p is the subject's projected area.

Using eq. (27) in eq. (21) and expressing D and $\cos\gamma$ as a function of x, y ,z, Θ, and Φ yields

$$dF_{P \to \mathrm{d}A} = \frac{1}{\pi} \frac{A_p}{A_r} \frac{y}{\sqrt{[(x \sin\Theta - z\cos\Theta\cos\Phi)^2 + (y - x\cos\Theta - z\sin\Theta\cos\Phi)^2 + (z\sin\Phi)^2]^3}} dA, \text{ with } dA = dx\, dz. \tag{28}$$

Therefore, view factor $F_{P \to \mathrm{d}A}$ can be obtained by integrating eq. (28), which, with the proper substitutions aimed at rendering the spatial variables non-dimensional, yields

$$F_{P\to A}=\frac{1}{\pi}\int_{\frac{x}{y}=0}^{\frac{x}{y}=\frac{a}{c}}\int_{\frac{z}{y}=0}^{\frac{z}{y}=\frac{b}{c}}\frac{f_p\sin\Theta\sin\Phi}{\sqrt{\left[\left(\frac{x}{y}\sin\Theta-\frac{z}{y}\cos\Theta\cos\Phi\right)^2+\left(1-\frac{x}{y}\cos\Theta-\frac{z}{y}\sin\Theta\cos\Phi\right)^2+\left(\frac{z}{y}\sin\Phi\right)^2\right]^3}}d\left(\frac{x}{y}\right)d\left(\frac{z}{y}\right),\quad(29)$$

where a is the width of surface A, b is its height, and c is its distance from the subject.

In Eq. (29) the projected area factor f_p can be determined with eq. (20) as a function of the azimuth α and altitude β angles, which may be properly evaluated with

$$\alpha=\arccos\frac{1-\frac{x}{y}\cos\Theta-\frac{z}{y}\sin\Theta\cos\Phi}{\frac{d}{y}};\ \beta=\arctan\frac{\frac{z}{y}\sin\Phi}{\frac{d}{y}},$$

$$\frac{d}{y}=\sqrt{\left(\frac{x}{y}\sin\Theta-\frac{z}{y}\cos\Theta\cos\Phi\right)^2+\left(1-\frac{x}{y}\cos\Theta-\frac{z}{y}\sin\Theta\cos\Phi\right)^2}.$$

5.2.2 View factors between human body and orthogonal rectangular surfaces

In the most common case of the view factor between the human body and orthogonal rectangular surfaces (Figure 7), eq. (29) can be simplified as

$$F_{P\to A}=\frac{1}{\pi}\int_{\frac{x}{y}=0}^{\frac{x}{y}=\frac{a}{c}}\int_{\frac{z}{y}=0}^{\frac{z}{y}=\frac{b}{c}}\frac{f_p}{\sqrt{\left[\left(\frac{x}{y}\right)^2+1+\left(\frac{z}{y}\right)^2\right]^3}}d\left(\frac{x}{y}\right)d\left(\frac{z}{y}\right)\quad(30)$$

with

$$\alpha=\arccos\frac{1}{d/y},\ \beta=\arctan\frac{z/y}{d/y}\ \text{and}\ \frac{d}{y}=\sqrt{\left(\frac{x}{y}\right)^2+1}.$$

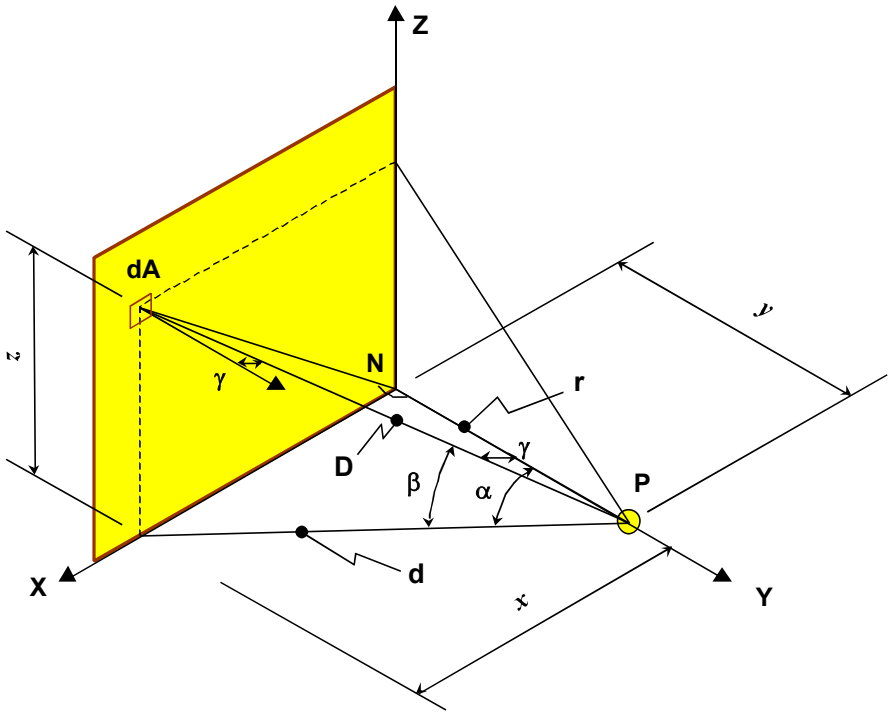

Figure 7. Reference system and geometrical parameters used for view factor assessment when the subject P is facing an orthogonal rectangular surface A.

5.2.3 Algorithms for composite surfaces

In the most frequently occurring situations in indoor environments, walls are composed of different elements such as doors, windows, heating panels and others. In these cases, the segment line linking the subject with the particular wall generally does not pass through the corner point of each of the elements composing the wall, which is the configuration allowing eqs. (29) and (30) to be applied. This fact entails that a manifold subdivision of the composite surfaces is generally needed in relation to the reciprocal position of each element.

Nevertheless, a general procedure aimed at surface partitioning can be designed, provided that significant points are suitably singled out. Therefore, referring to Figure 8, where P is the barycentre of the subject located in front of the wall, let point P′ be the orthogonal projection of P on the wall's plane, and let X'_P and Z'_P be its Cartesian coordinates. Moreover, let H and K be the left bottom and the right top corners of the surface, respectively, and let (X_H, Z_H) and $(X_K\ , Z_K)$ be their respective coordinates.

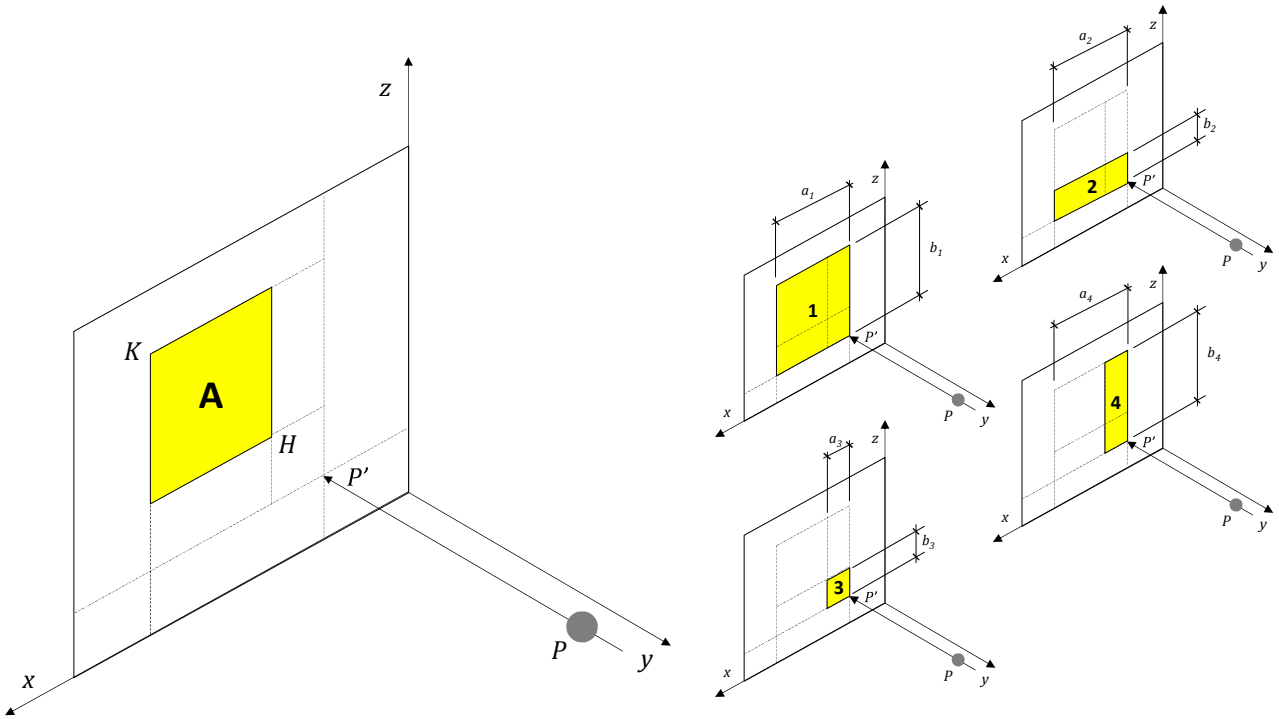

Figure 8. Geometric situations involving people and indoor surfaces: case of surface at the right side of the corner point P′.

In this frame, the view factor of surface A, suitable even when its corners are not aligned with the barycentre of the subject, is in turn placed in a generic point P of the room and can be computed by the following relationship (La Gennusa et al., 2007):

$$F_{P\to A} = \sum_{i=1}^{4} \frac{|a_i b_i F_{P\to i}|}{a_i b_i}, \tag{31}$$

where $F_{P\to i}$ is computed by the absolute values of parameters a_i and b_i which, in turn, may be calculated by the relationships reported in Table 3.

Table 3. Relationships for calculating parameters a_i and b_i.

i	***a***	***b***
1	$X_K - X_{P'}$	$Z_K - Z_{P'}$
2	$X_K - X_{P'}$	$Z_{P'} - Z_H$
3	$X_{P'} - X_H$	$Z_{P'} - Z_H$
4	$X_{P'} - X_H$	$Z_K - Z_{P'}$

5.2.4 Correction to be applied when the summation rule is not verified

The summation rule implies that the sum of the view factors from the surface of the subject to all surfaces of the surrounding environment must equal unity:

$$\sum_{i=1}^{N} F_{P\to i} = 1. \quad (32)$$

Occasionally, however, the calculation of view factors by eqs. (29) and (30) may lead to results which do not meet the condition expressed by eq. (32). In fact, the calculation procedures are not completely deterministic because they involve experimental data and regression analysis (e.g. regarding the projected factors; section 5.1). In this case, a correction must be applied. The difference to the unity can be proportionally shared among all computed view factors:

$$F_{P\to A}^{corr} = F_{P\to A} + \frac{1-\sum_{i=1}^{N} F_{P\to i}}{\sum_{i=1}^{N} F_{P\to i}} F_{P\to A} = F_{P\to A}\left(1 + \frac{1-\sum_{i=1}^{N} F_{P\to i}}{\sum_{i=1}^{N} F_{P\to i}}\right) = F_{P\to A}\left(\frac{\sum_{i=1}^{N} F_{P\to i}+1-\sum_{i=1}^{N} F_{P\to i}}{\sum_{i=1}^{N} F_{P\to i}}\right), \quad (33)$$

where $F_{P\to A}^{corr}$ is the corrected view factor.

Therefore, eq. (33) yields

$$F_{P\to A}^{corr} = \frac{F_{P\to A}}{\sum_{i=1}^{N} F_{P\to i}}. \quad (34)$$

6 Choosing algorithms and parameters for different situations

The choice of the pertinent algorithms and parameters involved in the equations used for MRT calculation essentially requires knowledge of the indoor environment layout, the subject's position inside the room, and both the HVAC system configurations and set-point values. This implies known or assessable information for all needed parameters including the temperatures of the internal surfaces of the environment, the angle factors among the opaque and glazed surfaces of the environment and the subject, the rate of high-intensity sources, the reflection coefficients of the indoor surfaces, the angle factors among the glazed and opaque surfaces of the environment, and the projected area factors of the subject.

In short, the proposed procedure can be subdivided into the following steps, as shown in Figure 9.

1. Design the building layout and system configuration (referred to as INPUT PHASE - DESIGN).
2. Design the indoor layout considering the human tasks to be performed inside the indoor environment. This leads to evaluation of a set of crucial input parameters and factors (referred to as INPUT PHASE - INPUT PARAMETERS):
    2a. Subject parameters;
    2b. Microclimatic parameters;
    2c. Inner surface temperatures;

2d. Heat source contribution, if any;

2e. Sun contribution, when present;

2f. Anthropometric parameters.

3. Assess the indoor radiative field and calculate the mean and plane radiant temperatures (referred to as INTERMEDIATE ASSESSMENT - RADIANT FIELD).
4. Assess the indoor comfort level (referred to as OUTPUT - GLOBAL COMFORT).
5. Assess the local discomfort occurrences (referred to as OUTPUT - LOCAL DISCOMFORT).

It is worth noting that although the procedure has been summarised as a sequence of steps for simplification, it is not merely intended to be a top-down process because the output of each step might lead to amendments regarding the former steps. For example, the results yielded at phase 3 might suggest changes to the layout design (phase 2) when considering changes in the position occupied by the subject. That is, the design procedure of the indoor thermal comfort is characterised by a feedback approach.

Furthermore, it is also noteworthy that phase 3, the core of the entire procedure, is a complex step involving a series of computations that for proper execution require selection of the appropriate algorithm depending on the physical phenomena occurring in the studied case. In addition, owing to the variability of the outdoor climate conditions, phase 3 might regard both the space and time domain, which entails the use of simulation tools to obtain the needed parameters, particularly at the design stage. In such a case, the temperatures of the internal surfaces of walls and windows constituting the building envelope, the variability of which is a function of external climate conditions, can be properly assessed only by using the above kind of tools.

To better clarify this procedure, the synoptic schemes reported in Tables 4 and 5 single out the proper algorithms and parameters to be adopted, depending on the specific case conditions. Moreover, because the methodology is essentially composed of a series of algorithms and parameters, the reliability of the procedure relies on the consistency of the assumptions of entire simulation. Therefore, these tables include the bibliographic references of papers validating the algorithms and parameters.

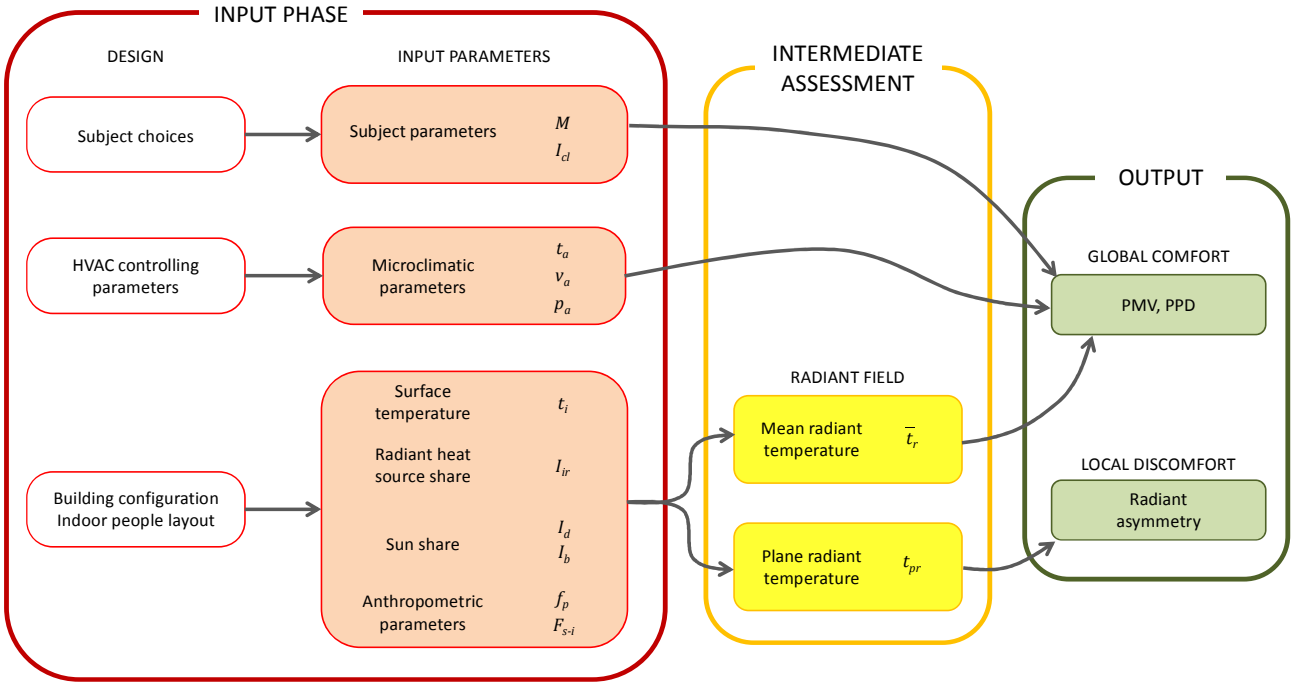

Figure 9. Scheme of the proposed procedure.

In short, the procedure involves a series of algorithms in which the complexity depends on the level of accuracy of the modelled radiative fluxes regarding the subject. This is accomplished by considering the relevant phenomena such as the presence of high-intensity sources and solar radiation among them, the geometrical configuration of the indoor environment such as orthogonal rectangular or tilted and rotated surfaces, and the temporal and spatial variations of the parameters. For energy- and economic-saving purposes, such complexity is unavoidable when pursuing the optimal layout design based on environmental use patterns.

Table 4. Synoptic scheme highlighting pertinent equations and parameters

Type of comfort assessment	Assessed parameter	Radiation striking the subject	Equation	Reference of validation	Relevant parameters
Global	Mean radiant temperature	Non-irradiated subject	(13)	(Fanger, 1970)	Envelope surface temperatures, T_i View factors between subject and opaque/glazed surfaces, $F_{S\to i}$
		Irradiated subject (high-intensity sources located inside the room)	(14)	(Fanger, 1970)	Envelope surface temperatures, T_i View factors between subject and opaque/glazed surfaces, $F_{S\to i}$ Projected area factor, f_p Radiant flux, I_{ir} Solar absorbance, α_{irr} Emittance of the person, ε_S
		Irradiated subject (solar radiation, no reflected components)	(15)	(La Gennusa et al., 2007)	Envelope surface temperatures, T_i View factors between subject and opaque/glazed surfaces, $F_{S\to i}$ Projected area factor, f_p Direct radiation striking the subject, I_b Diffuse radiation entering the room through glazed surface, I_d Solar absorbance, α_{irr} Emittance of the person, ε_S
		Irradiated subject (solar radiation - reflected components)	(16)	(Marino et al., 2017c)	Envelope surface temperatures, T_i View factors between subject and opaque/glazed surfaces, $F_{S\to i}$ Projected area factor, f_p Direct radiation striking the subject, I_b Diffuse radiation entering the room through glazed surface, I_d Direct radiation on the horizontal surface of the pavement, I_{bh} View factors between glazed and opaque

					surfaces, $F_{i\rightarrow j}$ Reflectance of the opaque surfaces, ρ Solar absorbance, α_{irr} emittance of the person, ε_S
Local	Plane radiant temperature	Non-irradiated subject	(17)	(Fanger, 1970)	Envelope surface temperatures, T_i View factors between the test area and the opaque/glazed surfaces, $F_{AT\rightarrow i}$
		Irradiated subject	(18)	Marino et al., 2017c)	Envelope surface temperatures, T_i View factors between the test area and the opaque/glazed surfaces, $F_{AT\rightarrow i}$ Diffuse radiation entering the room through glazed surface, I_d Direct solar radiation perpendicular to the test area, $I_{b\perp}$ Test area absorbance, α_{AT} Solar absorbance, α_{irr}

Table 5. Synoptic scheme highlighting equations for assessing anthropometric parameters.

Radiative human body factors	Situation	Equation	Reference of validation	Relevant parameters
Projected area factors	Irradiated subject	(20)	(Vorre, et al., 2015)	Azimuth angle, α (Figure 4) Altitude angle, β (Figure 4)
View factors	Tilted and rotated surfaces	(29)	La Gennusa et al., 2008)	Geometrical parameters (Figure 6)
	Orthogonal rectangular surfaces	(30)	(Fanger, 1970)	Geometrical parameters (Figure 7)
	Composite surfaces	(31)	Nucara et al., 1999)	Geometrical parameters (Figure 8)

7 Discussions

A discussion focused on the actual usefulness and applicability of the proposed equations and parameters is conducted in this section. A single room is considered (Figure 10) with a layout enabling easy description of the procedure including analysis of changes in time and space of the comfort conditions.

The internal dimensions of the module are 6.00 m × 6.00 m, whereas the floor-to-ceiling height is 3.00 m. Both north and west walls are adiabatic, as are as the floor and the roof; the south and east walls face the outdoor environment. The thermo-physical features (thermal transmittance U and internal capacity C) of the external walls are reported in Table 6. Two windows, 4.00 m × 1.20 m in areas, are installed on the south and east wall, respectively. Table 7 shows the main characteristics of the glazed surfaces without shading devices, including thermal transmittance U, solar transmittance τ_{sol}, visible transmittance τ_{vis}, and solar heat gain coefficient $SHGC$.

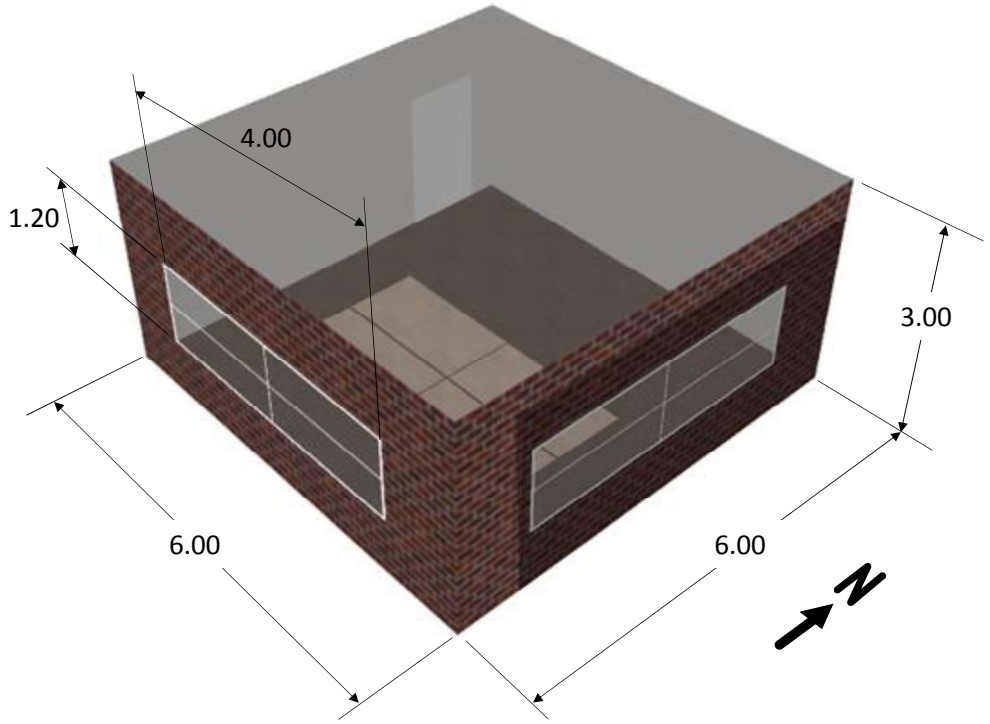

Figure 10. Perspective view of the case study building module.

Table 6. Thermo-physical features of external walls.

Thickness s (m)	**Thermal transmittance U (W/m^2K)**	**Frontal heat capacity C (kJ/m^2K)**
0.30	0.333	62.57

Table 7. Thermo-physical features of glazed surfaces.

Thermal transmittance U (W/m^2K)	**Solar transmittance τ_{sol}**	**Visible transmittance τ_{vis}**	**Solar heat gain coefficient SHGC**
1.785	0.498	0.668	0.619

This module is located in Palermo (Table 8), a town situated on the northern coast of Sicily and characterised by a typical humid subtropical climate profile with a hot summer and no dry seasons.

Table 8. Geographical coordinates and climatic characteristics of the selected city.

North latitude	**East longitude**	**HDD (18°C baseline)**	**CDD (18°C baseline)**	**Köppen climate classification** (Kottek et al., 2006)	**ASHRAE standard 196-2006 climate zone** (ASHRAE, 2016)
38°10′	13°6′	897	744	Cfa	3A

The indoor air conditioning was actuated by a variable air volume (VAV) system activated from 07:00 to 19:00 local time, which kept the air temperature within 20°C–26 °C.

Owing to the selected design choices, the effect on the indoor comfort conditions of the solar radiation entering the room through the two large windows cannot be disregarded. Thus, temporal and spatial changes of the environmental conditions must be considered, as described in Section 1. Energy simulation of the module was performed at the first stage of the analysis by using Energy Plus computer software (Crawley, 2001), and, the temperatures of the wall internal surfaces were obtained with an hourly time step. These values were exploited for MRT calculation.

To evaluate the spatial variability of the parameters, the floor surface of the room was patterned with a regular grid with a mesh size of 0.16 m × 0.16 m. The MRT values were assessed at every vertex of the described grid with an hourly time step by using eqs. (13) and (15), depending on whether the solar radiation directly reached the subject. This in turn involved the calculation of projected area factors (eq. (20)) given in Table 5, including view factors for orthogonal rectangular surfaces (eq. (30)) and those for composite surfaces (eq. (31)). The results of the described analysis are reported in Figures 11 and 12, which depict the isocurves of the MRT in the occupied area delimited by a boundary located 0.60 m from the envelope surfaces. Two specific days, June 21 and December 21, and three different times of day were considered: 8:00, 13:00 and 16:00.

It is worth noting that the areas directly irradiated by the sun, as delimited by the solid line in Figures 11 and 12, occurred at all three timers on the winter day (December 21) but only at 8:00 on the summer day (June 21). This occurred because the mean solar altitude is lower in winter than in summer; therefore, the solar rays are less effectively shielded by the building envelope. On the contrary, the higher solar altitudes, typical in the summer season, produced an irradiated zone on the floor of the room only at 8:00 owing to the presence of the east window. After that time, the solar altitude became too high, and the sun rays were shielded completely by the external walls.

8:00

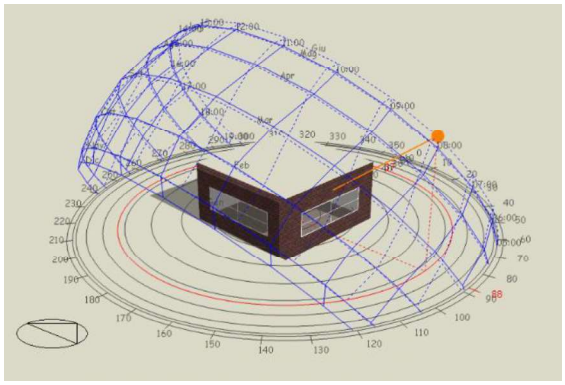

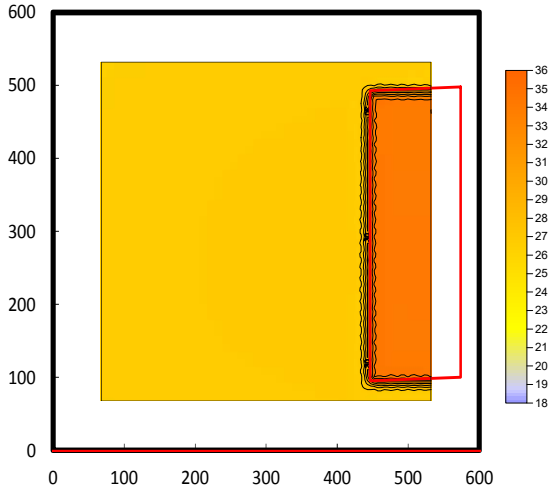

13:00

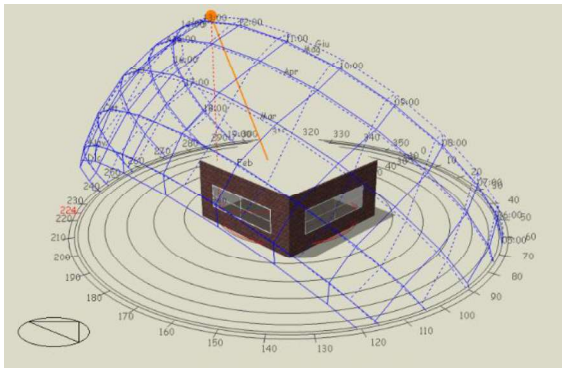

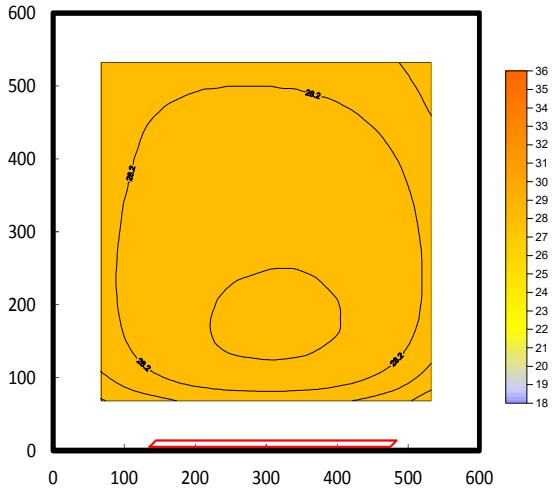

16:00

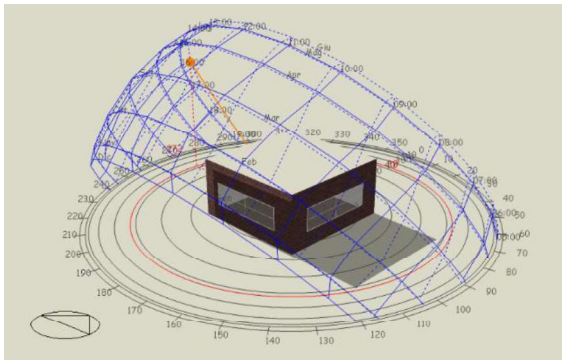

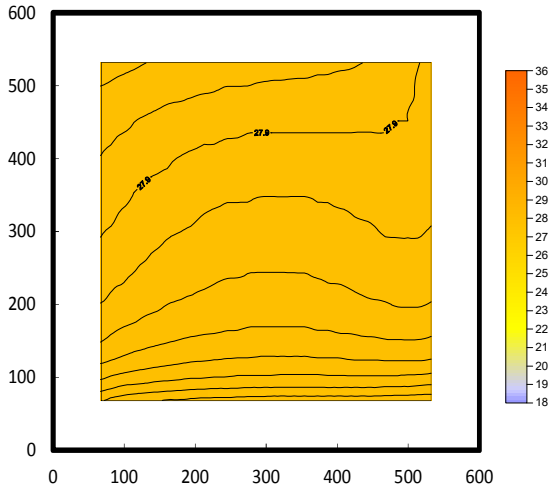

Figure 11. Isocurves of mean radiant temperature on June 21.

8:00

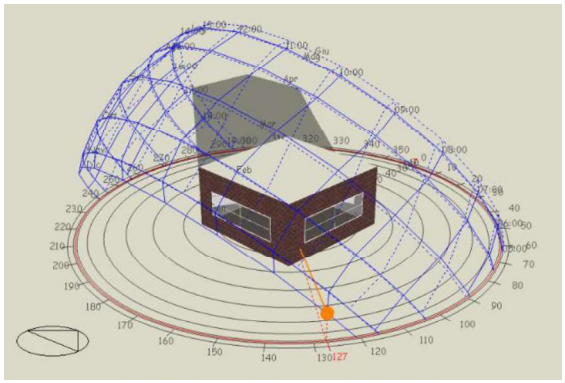

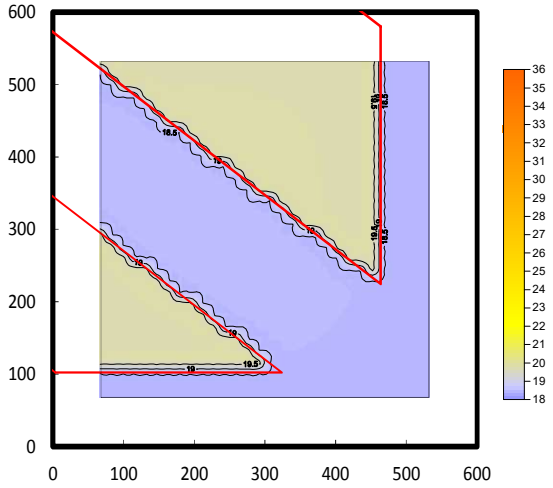

13:00

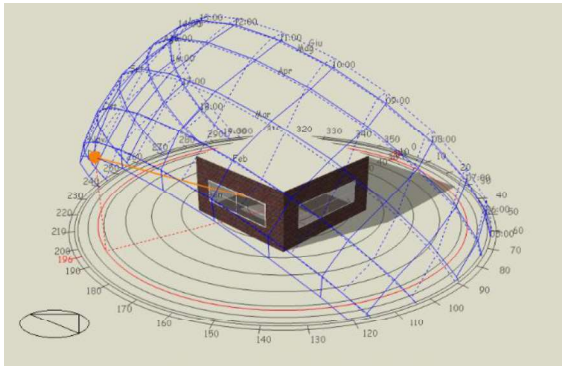

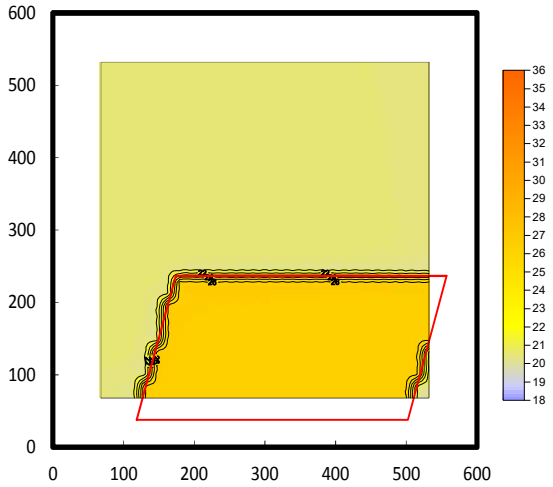

16:00

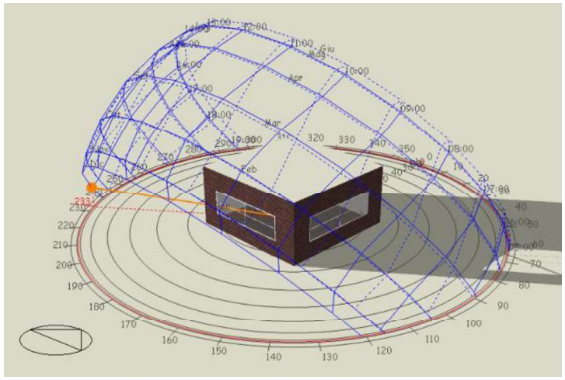

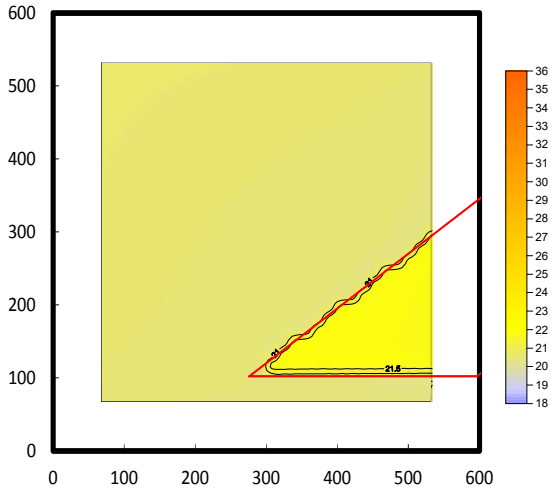

Figure 12. Isocurves of mean radiant temperature on December 21.

Regarding the indoor comfort conditions, Figure 13 reports the isocurves of PPD calculated for the subjective and environmental parameters indicated in Table 9.

Table 9. Environmental parameter configurations for comfort assessment.

Day of the year	M **(met)**	I_{cl} **(clo)**	RH **(%)**	v_a **(m/s)**
June 21	1.2	0.6	50	0.16
December 21		1.0		0.13

It is certainly relevant that although it increased the MRT values, the presence of the sun in winter slightly improved the level of comfort. In fact, at 8:00, the PPD decreased about 3%, from 12% to 9%, in the irradiated zones. At 13:00 and 16:00, however, the reduction was less than 1% and quite negligible, respectively. On the contrary, the irradiated zone appearance only at 8:00 in June is characterised by a PPD value of about 40% owing to a PMV value of +1.3. This value is significantly higher than the limit for acceptable environmental conditions, at 15%. Therefore, for the period during which the described condition persisted, this zone cannot be considered as comfortable for subjects. Such detailed representation of the indoor conditions represents a useful indication when designing suitable layouts of confined space or when planning effective HVAC systems aimed at limiting the discomfort occurrences inside the room.

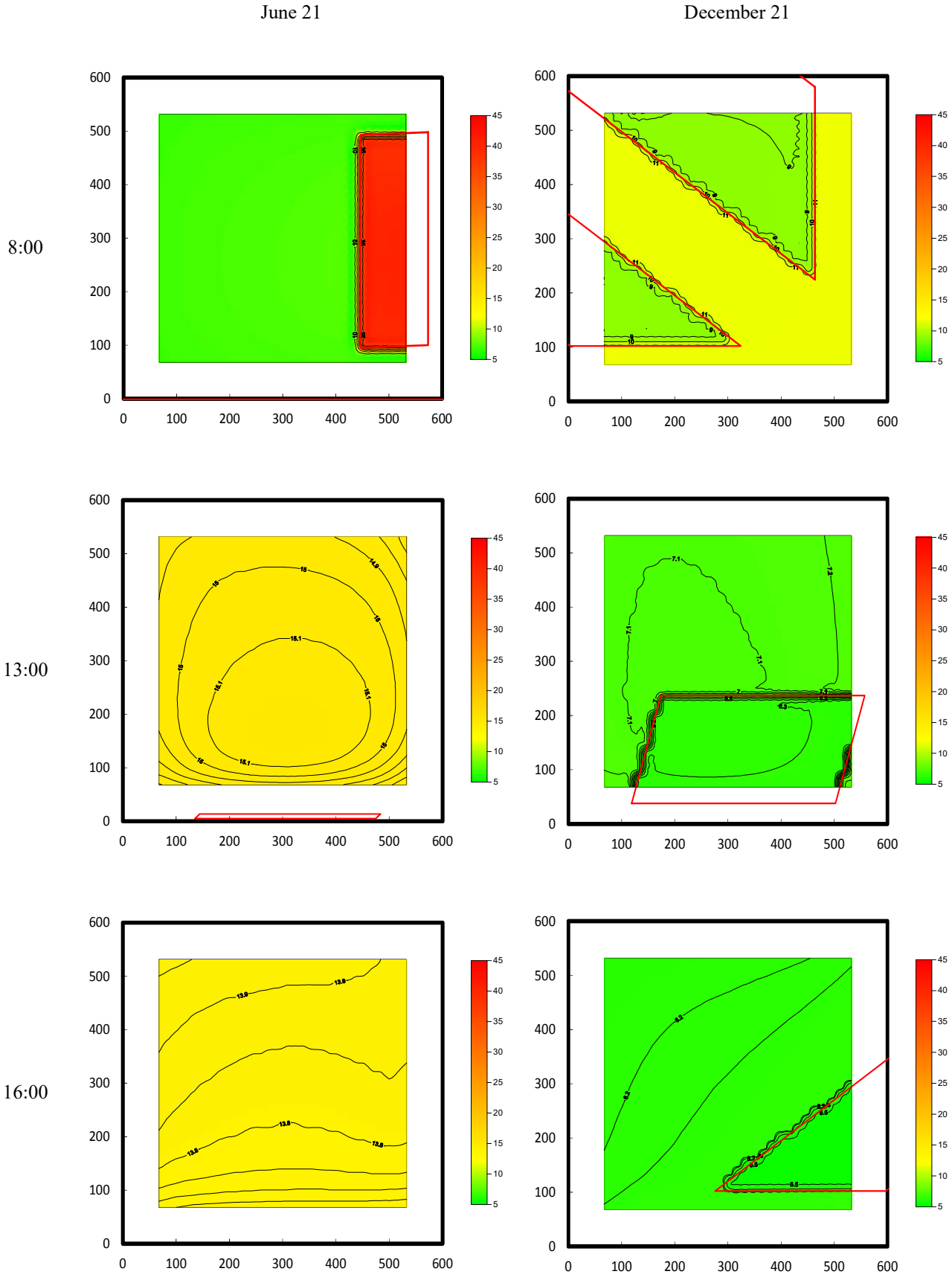

Figure 13. Isocurves of Predicted Percentage of Dissatisfied.

Regarding the time changes of parameters related to thermal comfort, the behaviours of MRT, PMV, and PPD were assessed at points P1(100; 300), P2 (300; 100) and P3 (500; 300), centred and located 100 cm from the north, south and east walls, respectively (Figure 14).

It can be inferred that the comfort levels may change locally with time to an extent that could be misleading if improperly assessed. For example, in June at point P3, the PMV progressively increases from +0.1 to +1.3 from 5:00 to 8:00 (Figure 15). Therefore, the thermal sensation shifted from 'neutral' to 'slightly warm' essentially because the solar radiation reached the considered position. Afterwards, the direct sun rays were shielded by the building envelope, and the PMV progressively decreased to +0.6.

In December, however, the PMV showed more fluctuation in time. At point P2, it ranged from a minimum value of -1.1, at 6:00 to a maximum value of +0.6, at 12:00. This can be attributed to the combined effects of the HVAC system, activated at 7:00, and of the presence of solar radiation, which reached the considered position from 8:00 to 12:00 with growing intensity and variable direction. In this case, the sun radiation shifted the thermal sensation of the occupants towards 'neutral' from 8:00 to 11:00. However, its increasing intensity can also contribute to worsening the comfort conditions, particularly when high irradiance values are reached such as that occurring at 12:00.

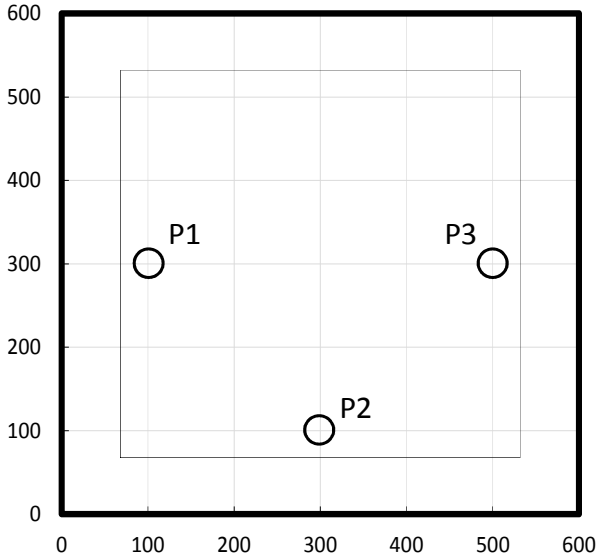

Figure 14. Positions of selected points P1, P2, and P3.

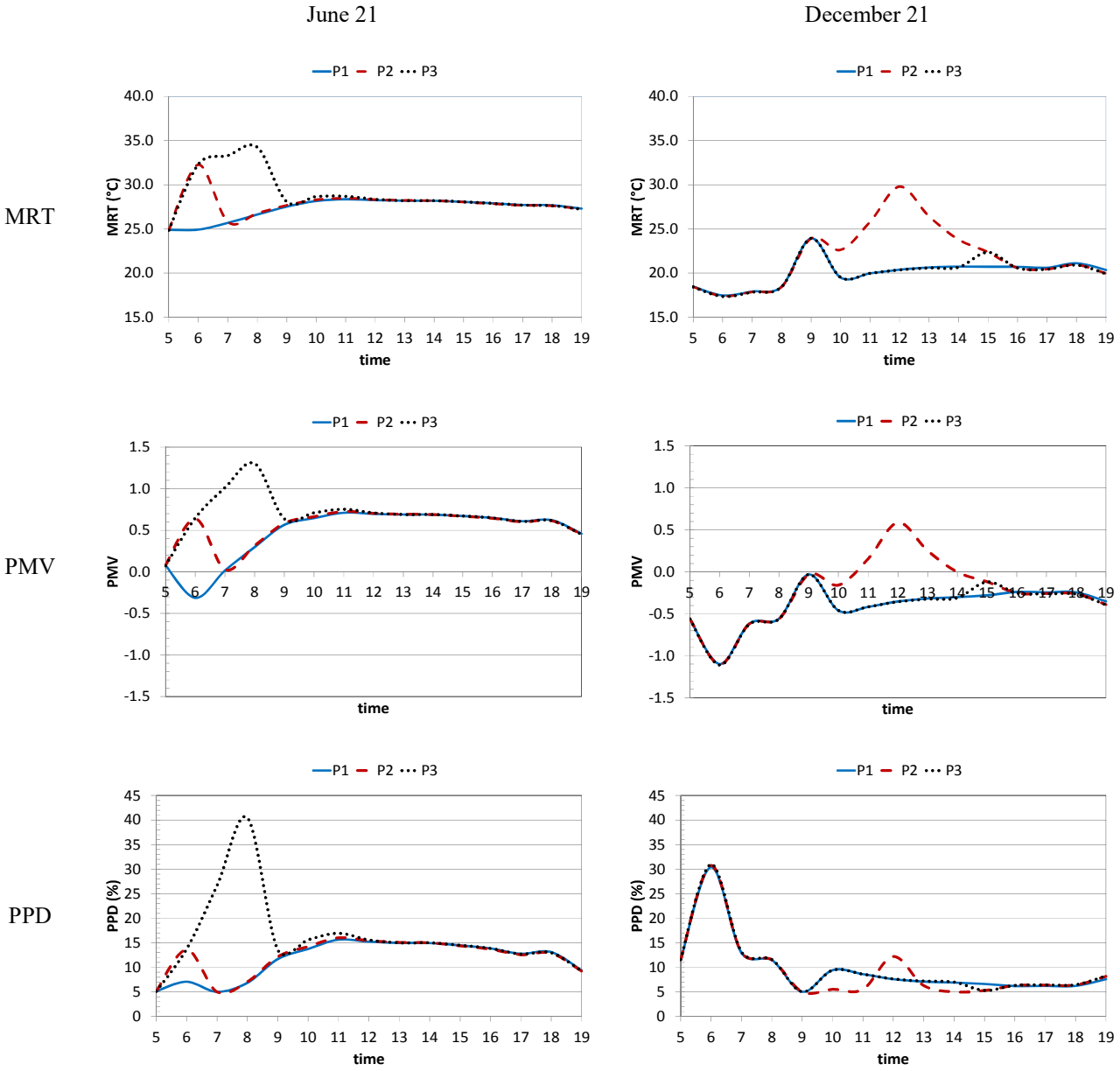

Figure 15. Time trends of mean radiant temperature (MRT) and Predicted Percentage of Dissatisfied (PPD) at points P1 (100; 300), P2 (300; 100), and P3 (500; 300).

In short, this example has shown that owing to the radiant fields, the indoor environmental conditions are characterised by space and time variability which cannot be neglected. During either the design or the management phases, incorrect consideration of this aspect can thus lead to inaccurate evaluation of the actual thermal environmental quality, resulting in the adoption of incorrect actions which could worsen the comfort level and energy efficiency of the HVAC system.

By properly patterning the physical phenomena which account for the described occurrences, the proposed methodology appears to be suitable for fulfilling both these purposes.

In addition, the described example demonstrates its efficacy in assessing the influence of important components of the envelope such as windows, the geometrical and thermo-physical features of which play a pivotal role in the heat exchange phenomena regarding the enclosed environment and in turn the occupants.

8 Conclusions

Optimal design of the thermal comfort conditions in confined spaces is a crucial issue for energy efficiency and for guaranteeing proper levels of environmental quality. In this context, detailed assessment of the indoor radiant field enveloping the human body is pivotal for accurate evaluation of the subject's thermal response. Moreover, the radiant field may vary in time and space for the effects of the building envelope configuration and the outdoor climate, which correspond to fluctuations in thermal sensations perceived by occupants.

This work introduced a comprehensive procedure enabling accurate assessment of the radiant field surrounding a subject in a realistic indoor environment considering variability in space and time along with the presence of high-intensity radiant sources. The proposed procedure consists of a set of analytical relations which can be used for computing all the needed anthropometric parameters. Moreover, they can be applied to complex building geometry and for assessment of MRT and radiant asymmetry. In this way, the effect of the building structure on thermal comfort can be assessed in correspondence of several different zones of the same room and during a particular time and not merely as an average condition in a given room.

The analysis presented in this study demonstrates the importance of considering space and time variability of the indoor environmental conditions owing to radiant fields. In fact, incorrect assessment of these variables during either the design or management phases might lead to misjudgement of the actual comfort levels in the room. Proper patterning of the physical phenomena which account for the described occurrences can be obtained by using the proposed methodology.

In addition, the proposed tool enables assessment of the influence of important components of the envelope such as windows, the geometrical and thermo-physical features of which play a pivotal role in the heat exchange phenomena regarding an enclose environment and in turn the occupants.

Therefore, the proposed algorithm serves as a contribution to enhance the accuracy of automatic computation of thermal comfort to enable a more realistic evaluation of the energy consumption for

climatisation purposes of buildings. Its feasibility for researchers and designers has been checked through application to a simple room model.

Useful indications for suitable design of layouts of confined space and evaluation of effective HVAC system size have also been presented to limit the discomfort perceived inside the room.

Acknowledgments

This work was carried out within the research project n. 201594LT3F, “La ricerca per i PAES: una piattaforma per le municipalità partecipanti al Patto dei Sindaci (Research for SEAP: a platform for municipalities taking part in the Covenant of Mayors)”, which is funded by the PRIN (Programmi di Ricerca Scientifica di Rilevante Interesse Nazionale) of the Italian Ministry of Education, University and Research.

References

Andersen, R., Fabi, V., Toftum, J., Corgnati, S.P., Olesen, B.W., 2013. Window opening behaviour modelled from measurements in Danish dwellings. Build. Environ. 69, 101–113. doi:10.1016/j.buildenv.2013.07.005.

Arens, E., Hoyt, T., Zhou, X., Huang, L., Zhang, H., Schiavon, S., 2015. Modeling the comfort effects of short-wave solar radiation indoors. Build. Environ. 88, 3–9. doi:10.1016/j.buildenv.2014.09.004.

ASHRAE, 1989. ASHRAE Handbook - HVAC Applications, American Society of Heating, Refrigerating and Air-Conditioning Engineers, Inc. Atlanta, GA.

ASHRAE, 2010. ANSI/ASHRAE Standard 55-2010. Thermal Environmental Conditions for Human Occupancy, (2010).

ASHRAE, 2016. Standard 90.1- Energy Standard for Buildings Except Low-Rise Residential Buildings.

Beccali, M., Nucara, A., Rizzo, G., 2004. Thermal comfort, in: Encycl. Energy, Elsevier Inc., Cleveland C. J., pp. 55–64.

Bianco, L., Cascone, Y., Goia, F., Perino, M., Serra., V. , 2017. Responsive glazing systems: Characterisation methods, summer performance and implications on thermal comfort. Sol. Energy. 158, 819-836.

Calvino, F., La Gennusa, M., Nucara, A., Rizzo, G., Scaccianoce, G., 2005. Evaluating human body area factors from digital images: A measurement tool for a better evaluation of the ergonomics of working places. Occup. Ergon. 5, 173–185.

CEN, 2007. EN 15251 - Indoor environmental input parameters for design and assessment of energy performance of buildings- addressing indoor air quality, thermal environment, lighting and acoustics.

Crawley, D.B., Lawrie, L.K., Winkelmann, F.C., Buhl, W.F., Huang, Y.J., Pedersen, C.O., et al., 2001. EnergyPlus: Creating a new-generation building energy simulation program. Energy Build. 33, 319–331. doi:10.1016/S0378-7788(00)00114-6.

D’Ambrosio Alfano, F.R., Palella, B.I., Riccio, G., 2011. The role of measurement accuracy on the thermal environment assessment by means of PMV index. Build. Environ. 46, 1361–1369. doi:10.1016/j.buildenv.2011.01.001.

D’Ambrosio Alfano, F.R., Olesen, B.W., Palella, B.I., Riccio, G., 2014. Thermal comfort: Design and assessment for energy saving. Energy Build. 81, 326–336. doi:10.1016/j.enbuild.2014.06.033.

Dell’Isola, M., Frattolillo, A., Palella, B.I., Riccio, G., 2012. Influence of measurement uncertainties on the thermal environment assessment. Int. J. Thermophys. 33, 1616–1632. doi:10.1007/s10765-012-1228-7.

European Parliament and the Council, 2010. Directive 2010/31/EU of The European Parliament and of the Council of 19 May 2010 on the energy performance of buildings (recast). Official Journal of the European Union L 153/13.

Fabi, V., Andersen, R.V., Corgnati, S., Olesen, B.W., 2012. Occupants' window opening behaviour: A literature review of factors influencing occupant behaviour and models. Build. Environ. 58, 188–198. doi:10.1016/j.buildenv.2012.07.009.
Fanger, P.O., 1970. Thermal comfort, Danish Technical Press, Copenhagen.
Fanger, P.O., Ipsen, B.M., Langkilde, G., Olessen, B.W., Christensen, N.K., Tanabe, S., 1985. Comfort Limits for Asymmetric Thermal Radiation. Energy Build. 8, 225–236. doi:10.1016/0378-7788(85)90006-4.
Fengzhi, L., Yi, L., 2005. Effect of clothing material on thermal responses of the human body. Model. Simul. Mater. Sci. Eng. 13, 809–827. doi:10.1088/0965-0393/13/6/002.
Fiala, D., Lomas, K., Stohrer, M., 2001. Computer prediction of human thermoregulatory and temperature response to a wide range of environmental conditions. Int. J. Biometeorol. 45, 143–159. doi:10.1007/s004840100099.
Fiala, D., Havenith, G., Bröde, P., Kampmann, B., Jendritzky, G., 2012. UTCI-Fiala multi-node model of human heat transfer and temperature regulation. Int. J. Biometeorol. 56, 429–441. doi:10.1007/s00484-011-0424-7.
Hodder, S.G., Parsons, K., 2006. The effects of solar radiation on thermal comfort. Int. J. Biometeorol. 51, 233–250. doi:10.1007/s00484-006-0050-y.
Horikoshi, T., Tsucjikawa, T., Kobayashi, Y., Miwa, E., Kurazumi, Y., Hirayama, K., 1990. The effective radiation area and angle factor between man and rectangular plane near him (Part II). ASHRAE Trans., 60–66.
Huizenga, C., Hui, Z., Arens, E., 2001. A model of human physiology and comfort for assessing complex thermal environments. Build. Environ. 36, 691–699. doi:10.1016/S0360-1323(00)00061-5.
ISO, 1998. ISO 7726 - Ergonomics of the thermal environment - Instruments for measuring physical quantities, International Standard Organization, Geneva.
ISO, 2001. EN ISO 13731 - Ergonomics of the thermal environment - Vocabulary and symbols, International Standard Organization, Geneva.
ISO, 2005. ISO 7730 - Ergonomics of the thermal environment - Analytical determination and interpretation of thermal comfort using calculation of the PMV and PPD indices and local thermal comfort criteria, International Standard Organization, Geneva.
Karlsen, L., Grozman, G., Heiselberg, P., Bryn, I., 2014. Operative temperature and thermal comfort in the sun - Implementation and verification of a model for IDA ICE, in: Indoor Air 2014 - 13th Int. Conf. Indoor Air Qual. Clim., pp. 200–207.
Katic, K., Zeiler, W., Boxem, G., 2014. Thermophysiological models: a first comparison, in: Fifth Ger. IBPSA Conf. RWTH Aachen Univ. Achen, Ger., pp. 595–602.
Kottek, M., Grieser, J., Beck, C., Rudolf, B., Rubel, F., 2006. World map of the Köppen-Geiger climate classification updated, Meteorol. Zeitschrift. 15, 259–263. doi:10.1127/0941-2948/2006/0130.
Kreith, F., Manglik, R.M., Bohn, M.S., 2011. Principles of Heat Transfer, 7th Edition, Cengage Learning, Inc, Stamford, CT 06902 USA.
La Gennusa, M., Nucara, A., Rizzo, G., Scaccianoce, G., 2005. The calculation of the mean radiant temperature of a subject exposed to the solar radiation—a generalised algorithm. Build. Environ. 40, 367–375. doi:10.1016/j.buildenv.2004.06.019.
La Gennusa, M., Nucara, A., Pietrafesa, M., Rizzo, G., 2007. A model for managing and evaluating solar radiation for indoor thermal comfort. Sol. Energy. 81, 594–606. doi:10.1016/j.solener.2006.09.005.
La Gennusa, M., Nucara, A., Pietrafesa, M., Rizzo, G., Scaccianoce, G., 2008. Angle Factors and Projected Area Factors for Comfort Analysis of Subjects in Complex Confined Enclosures: Analytical Relations and Experimental Results. Indoor Built Environ. 17, 346–360. doi:10.1177/1420326X08094621.
Marino, C., Nucara, A., Peri, G., Pietrafesa, M., Pudano, A., Rizzo, G., 2015a. An MAS-based subjective model for indoor adaptive thermal comfort. Sci. Technol. Built Environ. 21, 114-125. doi:10.1080/10789669.2014.980683.
Marino, C., Nucara, A., Pietrafesa, M., 2015b. Mapping of the indoor comfort conditions considering the effect of solar radiation. Sol. Energy. 113, 63–77. doi:10.1016/j.solener.2014.12.020.
Marino, C., Nucara, A., Pietrafesa, M., Polimeni, E., 2017a. The effect of the short wave radiation and its reflected components on the mean radiant temperature: modelling and preliminary experimental results. J. Build. Eng. 9, 42–51. doi:10.1016/j.jobe.2016.11.008.
Marino, C., Nucara, A., Pietrafesa, M., 2017b. Thermal comfort in indoor environment: effect of the solar radiation on the radiant temperature asymmetry. Sol. Energy. 144, 295–309.

doi:10.1016/j.solener.2017.01.014.
Marino, C., Misiani, P., Nucara, A., Pietrafesa, M., 2017c. The effect of the climatic condition on the radiant asymmetry. Int. J. Heat Technol. 35, 419-426. doi:10.18280/ijht.35Sp0157.
Miyazaki, Y., Saito, M., Seshimo, Y., 1995. A study of evaluation of non-uniform environments by human body model. J. Hum. Living Environ. 2, 92–100.
Nicol, J.F., Humphreys, M.A., 2002. Adaptive thermal comfort and sustainable thermal standards for buildings. Energy Build. 34, 563–572. doi:10.1016/S0378-7788(02)00006-3.
Nucara, A., Pietrafesa, M., Rizzo, G., Rodonò, G., 1999. Human body view factors for composite plane surfaces, in: Indoor Air 99, August 8th-13th 1999, Edinburg, Scotland, pp. 650–655.
Nucara, A., Pietrafesa, M., Rizzo, G., Scaccianoce, G., 2012. Handbook of Anthropometry, in: V.R. Preedy (Ed.), Handb. Anthr., Springer New York, pp. 91–114. doi:10.1007/978-1-4419-1788-1.
Parsons, K.C., 2014. Thermal Environments: The Effects of Hot, Moderate, and Cold Environments on Human Health, 3rd ed., Taylor & Francis, Boca Raton.
Rizzo, G., Franzitta, G., Cannistraro, G., 1991. Algorithms for the calculation of the mean projected area factors of seated and standing persons. Energy Build. 17, 221–230. doi:10.1016/0378-7788(91)90109-G.
Roulet, C.A., 2001. Indoor environment quality in buildings and its impact on outdoor environment. Energy Build. 33, 183–191. doi:10.1016/S0378-7788(00)00080-3.
Seppänen, O., Fisk, W.J., Lei-Gomez, Q., 2006. Room temperature and productivity in office work, in: Q. Lei (Ed.), Heal. Build. Conf., Lisbon, Portugal, pp. 243–247.
Stratbücker, S., Sumee, P., Bolineni, S.R., 2013. Efficient radiation simulation for thermal comfort. Bauphysik. 35, 30–37. doi:10.1002/bapi.201310039.
Tanabe, S.I., Kobayashi, K., Nakano, J., Ozeki, Y., Konishi, M., 2002. Evaluation of thermal comfort using combined multi-node thermoregulation (65MN) and radiation models and computational fluid dynamics (CFD). Energy Build. 34, 637–646. doi:10.1016/S0378-7788(02)00014-2.
Thellier, F., Monchoux, F., Bonnis-Sassi, M., Lartigue., B., 2008. Modeling additional solar constraints on a human being inside a room. Sol. Energy. 82, 290-301.
Vorre, M.H., Jensen, R.L., Le Dréau, J., 2015. Radiation exchange between persons and surfaces for building energy simulations. Energy Build. 101, 110–121. doi:10.1016/j.enbuild.2015.05.005.
Zhang, H., Huizenga, C., Arens, E., Wang, D., 2004. Thermal sensation and comfort in transient non-uniform thermal environments. Eur. J. Appl. Physiol. 92, 728–733. doi:10.1007/s00421-004-1137-y.